

Crystal-structure transformations and magnetic-ordering phenomena in $\text{GdCu}_{1-x}\text{Ga}_x$

J. C. M. van Dongen, T. T. M. Palstra, A. F. J. Morgownik, and J. A. Mydosh
Kamerlingh Onnes Laboratorium der Rijks-Universiteit, Leiden, The Netherlands

B. M. Geerken
Natuurkundig Laboratorium der Vrije Universiteit, Amsterdam, The Netherlands

K. H. J. Buschow
Philips Research Laboratories, Eindhoven, The Netherlands
(Received 8 February 1982; revised manuscript received 25 June 1982)

Electrical resistivity, magnetic susceptibility, thermal expansion, x-ray diffraction, and scanning calorimetry measurements have been performed over wide temperature ranges on the pseudobinary compounds $\text{GdCu}_{1-x}\text{Ga}_x$. In GdCu , which forms in the CsCl crystal structure at room temperature when prepared from the melt, a crystal-structure transformation into a low-temperature noncubic phase occurs at 250 K. Large hysteresis effects are observed with the transformation back into the CsCl structure occurring around 600 K, probably due to a stress-relieving process. In $\text{GdCu}_{1-x}\text{Ga}_x$ the CsCl crystal structure is stabilized for $x \geq 0.03$. The CsCl pseudobinary compound $\text{GdCu}_{1-x}\text{Ga}_x$ exhibits a kink-like anomaly in the magnetic susceptibility for $0.03 \leq x \leq 0.17$. This is ascribed to a complicated type of long-range antiferromagnetic ordering. For $0.17 < x < 0.29$ we suggest a mixed or canted low-temperature magnetic state for the ordered Gd moments. Over the whole $0.03 \leq x < 0.29$ concentration region a negative temperature coefficient is observed in the measured electrical resistivity at the ordering temperature. For $x \geq 0.29$ ferromagnetic long-range order is found. A simple model with only nearest-neighbor magnetic interactions, depending on the local Cu and Ga surroundings, is proposed to describe the x dependence of the paramagnetic Curie temperature. Finally a structural and magnetic phase diagram is constructed for the $\text{GdCu}_{1-x}\text{Ga}_x$ system with $0 \leq x \leq 0.5$.

I. INTRODUCTION

For a number of years now there has been considerable interest in intermetallic compounds of rare-earth elements (R) and nonmagnetic metals (M). The physical properties of these compounds have been recently reviewed by Buschow¹ and Kirchmayer and Poldy.² The majority of the equiatomic (1:1) RM compounds forms in the CsCl, CrB, or FeB crystal structure.³ In the RCu series the lighter R compounds attain the FeB structure, while in the heavier R compounds the CsCl structure is stable. GdCu is the first compound to form the CsCl structure at ambient temperatures. However, early work of de Wijn *et al.*⁴ reported a tendency for GdCu to transform into FeB structure at liquid-nitrogen temperature. After a suitable heat treatment the CsCl structure reappeared.⁴ Ross and Sigalas⁵ performed x-ray diffraction and Mössbauer effect measurements on GdCu powder down to 4.2 K, and their results were consistent with a stable

CsCl structure. Gefen and Rosen⁶ have very recently published electrical resistivity and dilatometry measurements on GdCu , both of which show a large temperature hysteresis. This indicates the occurrence of a structural phase transition. However, no additional corroborative evidence could be found via x-ray and metallographic techniques. They also determined the temperature dependence of the single crystal and polycrystalline elastic constants of GdCu between the ambient temperature and 77 K. These measurements revealed further evidence for a structural instability. Balster *et al.*⁷ reported a low-temperature structure transformation from the CsCl structure into the FeB and CrB structure in YCu , which is accompanied by a large temperature hysteresis in the electrical resistivity. Transformations from the cubic CsCl into the orthorhombic CrB and FeB structures have also been observed in several RPd and RAu compounds.^{8,9} For low transformation temperatures a large hysteresis between heating and cooling measurements is usually

observed.⁹ Magnetic susceptibility measurements by Debray *et al.*¹⁰ on YbAg and YbAu showed a transformation from the low-temperature FeB structure into the high-temperature CsCl structure at 777 and 772 K, respectively, however, only in YbAu is a large temperature hysteresis observed. Kimball *et al.*,¹¹ who performed Mössbauer effect measurements, found evidence for the coexistence of the FeB and CsCl phases at low temperatures in some RAu intermetallics. In LaAg_xIn_{1-x} a cubic-into-tetragonal transformation of the CsCl structure is observed.^{7,12} For $x < 0.2$ this transformation takes place with a large temperature hysteresis (~ 100 K).

The initial purpose of this investigation was to examine the concentration dependence of the magnetic properties in CsCl-type GdCu_{1-x}Ga_x compounds. These pseudobinary compounds were believed to be a favorable series for such study because of their simple crystal structure. Moreover, since Gd³⁺ is an *S*-state ion, there are no complications with crystalline field splitting of the degenerate magnetic ground state and no Kondo effect exists with Gd impurities. The GdCu_{1-x}Ga_x system is particularly interesting since high-temperature susceptibility measurements⁴ showed a variation of the paramagnetic Curie temperature Θ from negative to positive with increasing Ga concentration. For $x \simeq 0.15$ a vanishing value of Θ was observed so that, with a statistical distribution of Cu and Ga atoms, a spin-glass-like state might be formed at low temperatures. In the temperature region below 20 K Buschow *et al.*¹³ report results of heat-capacity measurements on GdCu_{1-x}Ga_x compounds having small or zero Θ values. No evidence was observed for magnetic ordering of any kind. The presence of large ferromagnetic, as well as large antiferromagnetic, Gd-Gd interactions in GdCu_{1-x}Ga_x for $x \simeq 0.15$ was then proposed¹³ to give rise to magnetic ordering at temperatures above 20 K. From low-temperature Mössbauer measurements on GdCu_{1-x}Ga_x and GdAg_{1-x}In_x Ross and Sigalas⁵ have suggested a decreasing density of *s*-like electrons in the conduction band with increasing x in both systems. This behavior is contrary to that expected in view of the *s-p*-type valence electrons of the Ga and In atoms. Energy-band calculations have been reported on YCu and YZn by Belakhovsky *et al.*¹⁴ and Hasegawa and Kübler.¹⁵ In both compounds a strong *4d* character is observed for the conduction electrons near the Fermi surface. In compounds of lanthanides instead of Y the same is expected to hold with respect to *5d* electrons, and

their character should play a large role in propagating the magnetic interactions. Very recently Köbler *et al.*¹⁶ have determined the magnetic phase diagram through magnetization measurements for GdAg_{1-x}Zn_x. Here the cubic CsCl structure is always present and a rather complicated mixture of magnetic phases seems to exist at low temperatures. Nevertheless, the following general trends do occur: an antiferromagnetic beginning at GdAg which changes over to complicated mixed phases around GdAg_{0.6}Zn_{0.4} and a ferromagnetic phase above about GdAg_{0.4}Zn_{0.6}. By comparison GdCu_{1-x}Ga_x has the Ga contributing one more conduction electron than the Zn. Therefore, one should expect a similar sort of phase diagram for GdCu_{1-x}Ga_x, but now with x reduced by approximately a factor of 2.

In this paper¹⁷ we present the results of measurements of the electrical resistivity, the low-field dynamic (ac) susceptibility, the static (4 kOe) susceptibility, and the thermal expansion of GdCu_{1-x}Ga_x. Results obtained with scanning calorimetry, x-ray diffraction, and photomicrograph examinations are also reported. In addition we have also studied the related compounds YCu_{1-x}Ga_x, Gd_{1-y}R_yCu ($R = \text{Sm or Tm}$), and Gd_{1-y}Y_yCu_{0.9}Ga_{0.1}. Through these experiments a picture is obtained of the crystal-structure transformations, which strongly influence the magnetic properties. For the stable CsCl pseudobinaries we have examined the magnetic ordering phenomena and propose a simple model to describe them. The present paper is organized as follows. In Sec. II we give the experimental details of our sample preparation and measuring techniques. Section III contains and compares the experimental results. In Sec. IV our results are discussed and contrasted with experimental evidence on other equiatomic compounds of rare earths and nonmagnetic metals. A brief summary and some conclusions are presented in Sec. V.

II. EXPERIMENTAL DESCRIPTION

The samples were prepared by arc melting in an atmosphere of purified argon gas. The starting material purities were 99.9% for the rare-earth metals, 99.99% for copper, and 99.99% for gallium. It was previously shown by room-temperature x-ray diffraction analysis^{4,13,17} that the CsCl-type phase was the main phase present in GdCu_{1-x}Ga_x for $x \leq 0.5$ with the amount of impurity phases estimated to be less than a few percent. All other compounds

prepared for the present study also attain the CsCl crystal structure at room temperature. It should be noted here that low-temperature ($T < 300$ K) structural phase transformations with large hysteresis are involved in our investigations.

In the temperature region between 2 and 300 K the electrical resistivity was measured via a standard four-point probe technique with a dc current of 10 mA, constant to a few ppm, and a voltage determination accurate to about 2 parts in 10^5 . The resistivity samples, which were prepared by spark erosion from the bulk, had typical dimensions of $1 \times 1 \times 15$ mm³. The temperature was varied stepwise in both the heating and cooling directions and determined to within 0.2% using calibrated Ge and Pt resistors. The error of the measured absolute resistivity was about 2% due to uncertainties in the sample dimensions.

For temperatures above room temperature up to 750 K the electrical resistivity was also measured with a spot-welded four-point contact technique. Here the dc current was 50 mA, constant to one part in 10^4 , and the voltage determination was accurate to about one part in 10^3 . By using an electric furnace the temperature, which was determined by a calibrated Pt resistor, was varied continuously, but not faster than 2 deg/min. The sample was mounted near the Pt resistor in a stainless-steel tube, which was continuously evacuated to 10^{-5} Torr by an oil diffusion pump. With this method the temperature determination was accurate to within a few degrees.

The static susceptibility χ_s was measured with a sensitive pendulum magnetometer¹⁸ in the temperature region between 4 and 300 K. The magnetic field gradient required in this method is produced by spherical pole shoes of an electromagnet. This symmetric field gradient produces a force on the sample which is determined by measuring the change in oscillation frequency of the pendulum on which the sample is attached. Measurements were usually performed in a field of about 4 kOe. The accuracy of the measured susceptibility was to well within $\pm 1\%$. A calibrated Au-0.03% Fe versus Chromel thermocouple was used to determine the temperature over the entire region.

The dynamic (ac) susceptibility χ_d was measured using the standard combination of a primary coil producing a driving ac field of 1 Oe at a frequency of 140 Hz and two compensated secondary coils for the detection of the sample response. Here the temperature region studied was usually between 2 and 100 K, with an extension to higher temperatures for

a small number of samples. The temperature was determined using calibrated glass-carbon and Pt resistors. There was no compensation for the earth's magnetic field so a static field of $\sim \frac{1}{2}$ Oe was present at the sample. For both types of susceptibility measurements 3-mm-diameter spheres were formed by spark erosion.

The thermal-expansion measurements were carried out by means of a three-terminal capacitance technique using a General Radio 1621 bridge. For GdCu we used a dilatometer similar to that described by Brändli and Griessen.¹⁹ The length changes are determined relative to Berylco 25 from which the dilatometer is constructed. The thermal expansion of GdCu_{0.9}Ga_{0.1} was determined by means of the same capacitance technique but relative to YCu_{0.9}Ga_{0.1} using a differential dilatometer. Temperature variation was achieved in an Oxford Instruments continuous-flow cryostat and was measured with a Pt resistor calibrated to an accuracy of better than 0.5 K.

Scanning calorimetry studies were carried out below room temperature in a helium atmosphere using a Perkin and Elmer 1B scanning calorimeter. The temperature recording is accurate to within 1 K and the latent heat determination to within 0.05 cal/g.

In order to determine the crystal-structure parameters a series of Bragg diffraction measurements was performed. For low-temperature measurements a cryostat could be installed in the x-ray apparatus. In all our x-ray experiments Cu $K\alpha$ radiation ($\lambda = 1.541838$ Å) was used. This consists of $K\lambda_1$ ($\lambda = 1.540562$ Å) and $K\lambda_2$ ($\lambda = 1.544390$ Å) radiation with relative intensities 2 and 1, respectively. For calibration of the diffraction angles the sample was mounted together with Si powder. In the temperature region between 5 and 300 K a number of Bragg diffraction spectra were taken from the surface of bulk GdCu. Before mounting in the goniometer the sample was mechanically polished to remove surface oxidation. We also performed room-temperature Bragg diffraction measurements on a bulk GdCu sample with various thermal histories. In addition to these room-temperature x-ray experiments, we also examined the sample surface under a metallurgical microscope with magnifications up to 1000. To study surface effects a thin surface layer (~ 0.2 mm) was removed from a GdCu sample at 77 K by filing. During the filing the sample was kept under liquid nitrogen. Then a room-temperature Bragg diffraction spectrum was taken on the bulk sample. In another experiment

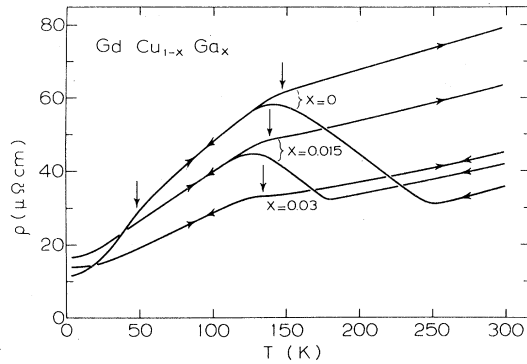


FIG. 1. Electrical resistivity vs temperature for $\text{GdCu}_{1-x}\text{Ga}_x$ with $0 \leq x \leq 0.03$. The arrows on the resistivity curves denote the measuring direction. The vertical arrows indicate the magnetic ordering temperatures.

GdCu was crushed into powder under liquid nitrogen and then a Bragg diffraction spectrum was measured at room temperature. For comparison the same experiment was performed on NdCu which is known to possess the FeB structure. We also performed x-ray experiments on bulk $\text{GdCu}_{0.94}\text{Ga}_{0.06}$. After polishing to remove surface oxidation, the sample was strain annealed at 500°C in vacuum for 2 h. Bragg diffraction spectra were measured at room temperature and liquid-nitrogen temperature, and the sample surface was inspected under the microscope at room temperature.

III. EXPERIMENTAL RESULTS

A. Electrical resistivity

In Fig. 1 we show the measured total resistivities $\rho(T)$ versus temperature of $\text{GdCu}_{1-x}\text{Ga}_x$ for Ga concentrations $0 \leq x \leq 0.03$. Experimentally the sample was first cooled from room temperature to liquid-helium temperatures and then heated to room temperature again, as indicated by the arrows on the resistivity curves.

For GdCu ($x=0$), we observe a normal, positive $d\rho/dT$ temperature dependence down to 250 K. In the temperature region from 250 to 130 K a negative $d\rho/dT$, and, moreover, time-dependent effects were found. Even after stabilizing the sample at a given temperature, the measured resistivity increased about $2 \mu\Omega \text{ cm}$ in the first few minutes and then became constant. We did not further take into account this relatively small time effect in the resistivity versus temperature curves. On cooling below 130 K to liquid-helium temperatures, a "knee"-like anomaly is observed at 48 K, as indicated by a vertical

arrow in Fig. 1. Upon reheating the sample, a considerable hysteresis was found above 130 K. At 148 K, a second "knee"-like anomaly is observed, also denoted by a vertical arrow, which is followed at higher temperatures by a normal positive $d\rho/dT$ dependence, in strong contrast to the negative $d\rho/dT$ found upon cooling the sample.

When substituting Ga for Cu ($x=0.015$), the resistivity hysteresis diminishes, and the onset of the negative $d\rho/dT$, at 250 K for GdCu , is shifted to lower temperatures. For $x=0.03$, the resistivity hysteresis has disappeared and the $\rho(T)$ curve is completely reversible. The kneelike anomaly, at 148 K for GdCu , moves slightly to lower temperatures with increasing x (see Fig. 1), and gradually transforms its character to a reversible "dimple" in the measured resistivity. The 48-K anomaly becomes less pronounced with increasing Ga concentration and has disappeared for $x=0.03$.

Figure 2 shows some of our resistivity versus temperature curves of $\text{GdCu}_{1-x}\text{Ga}_x$ at higher Ga concentrations. A fully reversible negative $d\rho/dT$

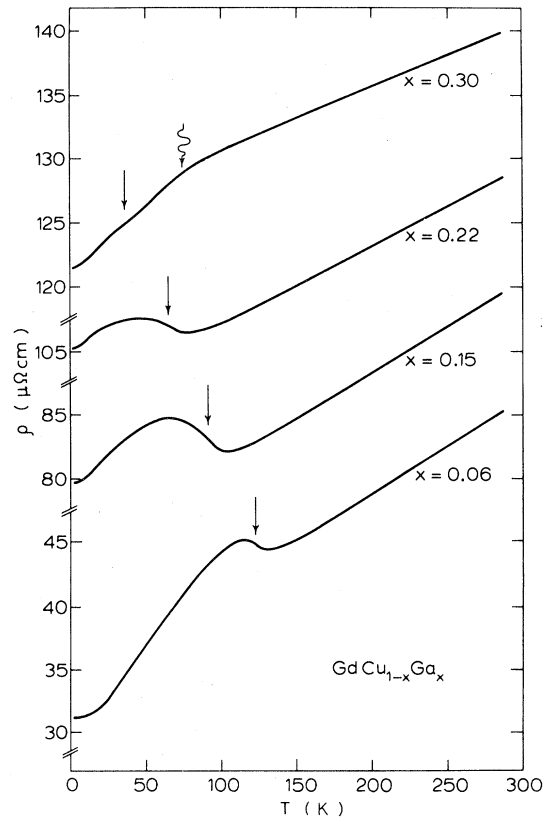


FIG. 2. Electrical resistivity vs temperature for $\text{GdCu}_{1-x}\text{Ga}_x$ with $0.06 \leq x \leq 0.30$. The arrows indicate the magnetic ordering temperatures.

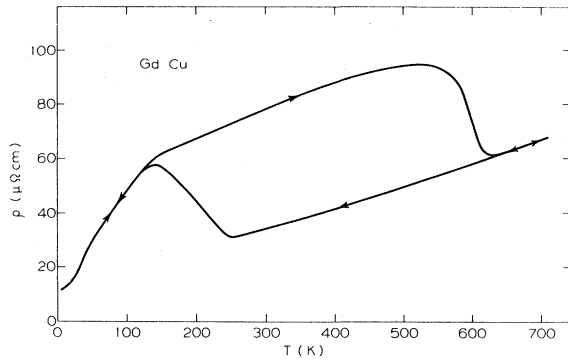


FIG. 3. Electrical resistivity vs temperature for GdCu. The arrows on the resistivity curves denote the measuring direction.

contribution to the measured resistivity, already present for $x=0.03$ when the positive phonon contribution is considered, can be clearly observed and followed up to $x=0.30$. The temperatures of minimum $d\rho/dT$ are indicated by arrows in the figure. For $x=0.30$, in addition, a kneelike anomaly is present at a somewhat higher temperature, denoted by the wavy arrow in Fig. 2.

The resistivity versus temperature behavior was also measured for four pseudobinary $\text{Gd}_{1-y}\text{Y}_y\text{Cu}_{0.9}\text{Ga}_{0.1}$ compounds with $0 \leq y \leq 1$. All these compounds showed no resistivity hysteresis. The negative $d\rho/dT$ dependence present for $y=0$ (see the resistivity results on $\text{GdCu}_{1-x}\text{Ga}_x$ in Fig. 2) gradually decreases in magnitude and temperature with decreasing Gd concentration.

The $\rho(T)$ behavior for $\text{Gd}_{0.9}\text{Sm}_{0.1}\text{Cu}$ and $\text{Gd}_{0.9}\text{Tm}_{0.1}\text{Cu}$ was also determined and is basically similar to GdCu except for a shift of the second kneelike anomaly on the heating curve to lower temperatures and an increase (decrease) of the ρ hysteresis for Sm (Tm). In addition, the two non-magnetic systems YCu and $\text{YCu}_{0.97}\text{Ga}_{0.03}$ were measured. Here the magnetic anomalies in the resistivity are absent and the ρ hysteresis disappears with the substitution of $x=0.03$ Ga exactly as in $\text{GdCu}_{1-x}\text{Ga}_x$.

Resistivity measurements above room temperature have been performed on GdCu, $\text{Gd}_{0.95}\text{Tm}_{0.05}\text{Cu}$, and $\text{GdCu}_{0.985}\text{Ga}_{0.015}$. As mentioned above all these materials show a considerable hysteresis at low temperatures. Here the starting material was always the temperature-cycled (300 K \rightarrow 2 K \rightarrow 300 K) sample. In the high-temperature experiments the sample was first heated to about 700 K and then cooled back to 300 K. As a typical example of the high-temperature resistivity we show

in Fig. 3 the behavior for GdCu combined with the low-temperature result from Fig. 1. On increasing the temperature, a strong negative $d\rho/dT$ dependence is observed around 600 K, followed at higher temperatures by a normal, positive $d\rho/dT$ behavior. The temperature where the resistivity hysteresis has disappeared is 636 K for GdCu. When recoiling the sample this positive $d\rho/dT$ dependence is followed and maintained down to 300 K, where within the experimental accuracy the low- and high-temperature resistivity measurements match nicely. For $\text{Gd}_{0.95}\text{Tm}_{0.05}\text{Cu}$ and $\text{GdCu}_{0.985}\text{Ga}_{0.015}$ quite similar resistivity versus temperature curves are obtained and the resistivity hysteresis disappears at the temperatures 618 and 642 K, respectively.

B. Magnetic susceptibility

In Fig. 4 we plot the inverse of the static susceptibility χ_s^{-1} versus temperature as measured on GdCu. In this experiment the temperature was varied from room temperature to liquid-helium temperatures and then back again to room temperature. Similar to the resistivity curves for GdCu a considerable hysteresis is also observed in $\chi_s(T)$. When cooling the sample, χ_s^{-1} varies linearly with temperature down to 232 K. Below 232 K the hysteresis in χ_s^{-1} decreases with decreasing temperature and vanishes at 125 K. By lowering the temperature further, a shallow minimum is observed at 48 K. Upon heating the sample from 4 K, a linear variation of χ_s^{-1} with temperature develops above 140 K. In both linear regions, above 232 K on cooling and above 140 K on heating, the sample is clearly in the paramagnetic state, and, by extrapolation

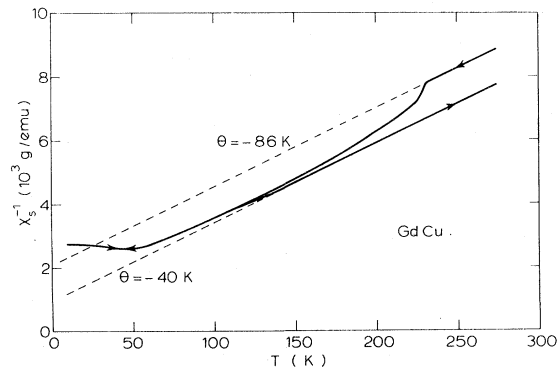


FIG. 4. Inverse of the static susceptibility vs temperature for GdCu. The arrows on the susceptibility curves denote the measuring direction.

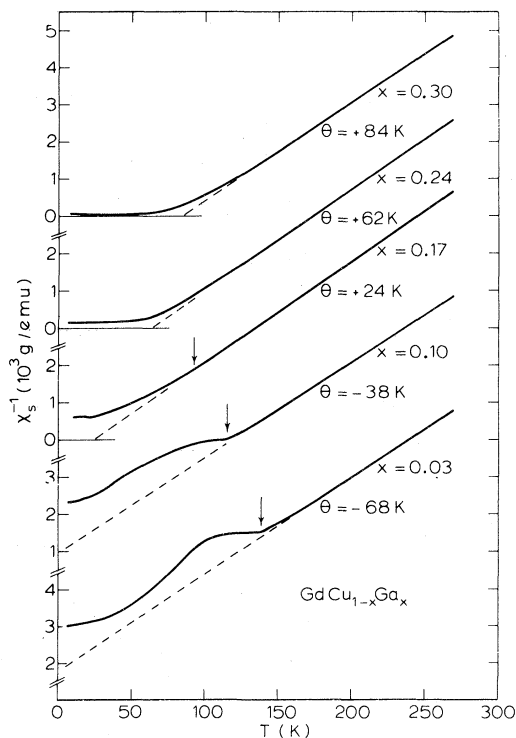


FIG. 5. Inverse of the static susceptibility vs temperature for $\text{GdCu}_{1-x}\text{Ga}_x$ with $0.03 \leq x \leq 0.30$. The arrows indicate the magnetic ordering temperatures.

tion, paramagnetic Curie temperatures $\Theta = -86$ K and -40 K are obtained.

We collect in Fig. 5 some typical χ_s^{-1} versus temperature curves for five $\text{GdCu}_{1-x}\text{Ga}_x$ samples with $0.03 \leq x \leq 0.30$. In this susceptibility experiment the samples are cooled to liquid-helium temperatures within a few minutes and then measured with increasing temperature. Since for these x values the resistivity $\rho(T)$ exhibits no hysteresis, we do not expect any hysteresis in the magnetic susceptibility. At high temperatures all samples are in the paramagnetic state, and via extrapolation the paramagnetic Curie temperature Θ is obtained. A gradual variation from $\Theta = -68$ K for $x = 0.03$ to $\Theta = +84$ K for $x = 0.30$ is observed. In the paramagnetic region an effective moment per Gd atom p is obtained from the slope of χ_s^{-1} versus temperature. For all Ga concentrations a p value is obtained which is a few percent higher than the free-ion value $7.94\mu_B$ for Gd^{3+} . For $x \geq 0.03$, "kinklike" anomalies are observed in χ_s^{-1} , which with increasing Ga-concentration shift to lower temperatures and become less pronounced. The kinklike anomalies are indicated by arrows in Fig.

5. At $x = 0.17$ the anomaly becomes submerged in the large susceptibility values which occur at low temperatures. For $x > 0.17$, more gradual deviations from paramagnetic behavior are observed which begin at higher temperatures as the Ga concentration is increased. At low temperatures ($T \leq 50$ K) the susceptibility χ_s increases with increasing x in the full $0.03 \leq x \leq 0.30$ range.

In Fig. 6 we plot some typical curves of the low-field (driving field ~ 1 Oe) dynamic susceptibility χ_d versus temperature for $\text{GdCu}_{1-x}\text{Ga}_x$ with $0 \leq x \leq 0.3$ as measured in the temperature region between 2 and 100 K. For all Ga concentrations a broad maximum which is strongly dependent on the driving field is observed around 40 K. At low temperatures ($T < 40$ K) a shoulder develops, which with increasing Ga concentration increases in magnitude and shifts to higher temperatures. For $x = 0.30$ a cusplike anomaly is observed at 38 K.

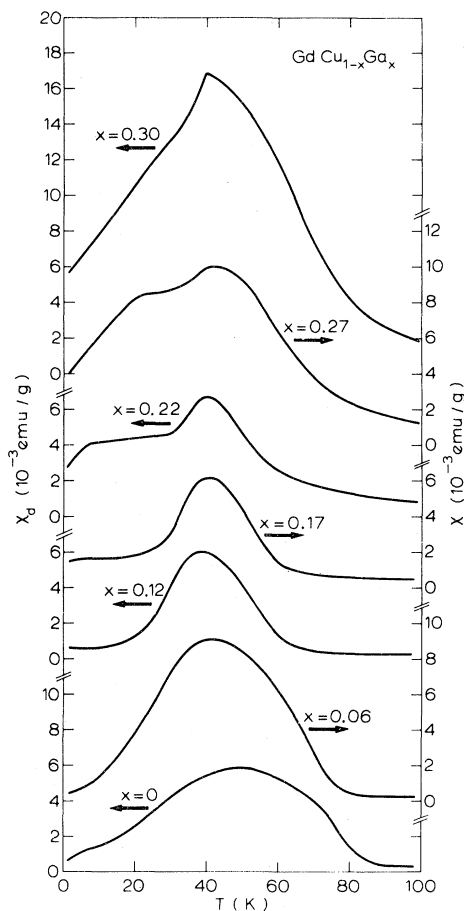


FIG. 6. Dynamic (ac) susceptibility vs temperature for $\text{GdCu}_{1-x}\text{Ga}_x$ with $0 \leq x \leq 0.3$.

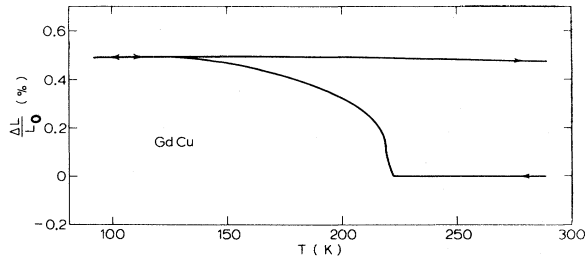


FIG. 7. Length change vs temperature for GdCu. The arrows on the curves denote the measuring direction.

These χ_d (1 Oe) results are quite different from the χ_s (4 kOe) shown in Fig. 5. At low temperatures ($T < 100$ K) a large field dependence is observed in the measured susceptibilities. Here

$$\chi_d \equiv \left. \frac{\partial M}{\partial H} \right|_{H \rightarrow 0} \neq \chi_s \equiv \frac{M}{H},$$

where $H = 4$ kOe. Especially for the lower Ga concentrations, a strong enhancement of χ_d relative to χ_s is observed around 40 K. With increasing Ga concentration the enhancement of χ_d diminishes. The application of a static magnetic field of typically 100 Oe, parallel to the ac driving field of 1 Oe, was sufficient to suppress the strong enhancement in χ_d . The results of the χ_d versus temperature measurements on $\text{GdCu}_{1-x}\text{Ga}_x$ performed above 100 K agree fully with $\chi_s(T)$. Also in χ_d kinklike anomalies were observed for the lower Ga concentrations.

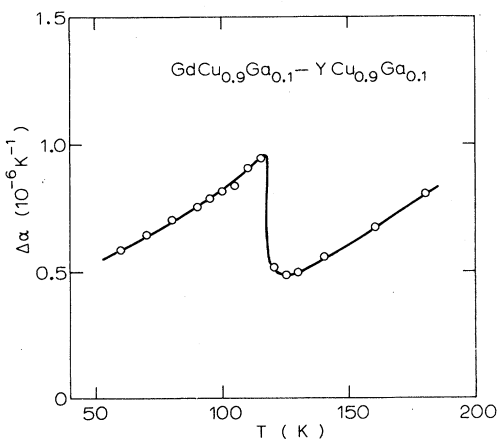


FIG. 8. Temperature dependence of the thermal-expansion coefficient for $\text{GdCu}_{0.9}\text{Ga}_{0.1}$ relative to $\text{YCu}_{0.9}\text{Ga}_{0.1}$

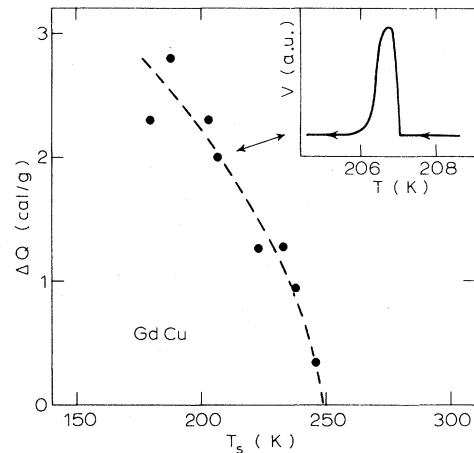


FIG. 9. Latent heat vs (structural) transition temperature for GdCu. The dashed line serves as a guide for the eye. In the inset a scanning calorimeter voltage vs temperature measurement is plotted as a typical example. The measuring direction is denoted on the curve and the double arrow indicates the associated $\Delta Q(T_s)$.

C. Thermal expansion and scanning calorimetry

The length change $\Delta L/L_0$ of GdCu versus the temperature is given in Fig. 7. Here the sample was cycled from 293 to 95 K and back to 293 K again, as denoted by the arrows on the curves. Similar to the resistivity and susceptibility behavior, a hysteresis was also observed as an irreversible length change of 0.5% upon cooling down below 221 K down to 124 K. Note that the length change was measured relative to Berylco 25, which results in the nearly constant $\Delta L(T)/L_0$ behavior apart from the irreversible length change. A second experiment shown in Fig. 8 plots the temperature dependence of the thermal-expansion coefficient $\Delta\alpha = (d/dT)(\Delta L/L_0)$ for $\text{GdCu}_{0.9}\text{Ga}_{0.1}$ relative to $\text{YCu}_{0.9}\text{Ga}_{0.1}$. A rather sharp steplike anomaly in $\Delta\alpha$ is observed at 118 K, which is fully reversible in temperature. Note for comparison that the linear expansion coefficient α for GdCu at room temperature is typically 10^{-5} K^{-1} .

Figure 9 (inset) plots the scanning calorimeter voltage versus temperature for a typical GdCu sample. The measurement was performed with decreasing temperature as indicated. The observed anomaly is characteristic for a first-order phase transition, and the area reveals the associated latent heat ΔQ . Note that the anomaly is only 1-K wide in temperature. Further scanning calorimetry measurements

were performed on several different GdCu samples. From these measurements we can determine the latent heat ΔQ which is plotted versus the observed transition temperature T_s in Fig. 9. For each measurement the GdCu starting material was in the high-temperature phase. On samples which had already been measured at low temperatures, a 500°C heat treatment was performed prior to the next low-temperature measurement. When this 500°C heat treatment was performed in a He atmosphere, relatively low transition temperatures and high ΔQ values were obtained ($\Delta Q \geq 2$ cal/g). For GdCu samples measured directly after casting or on which the 500°C heat treatment was performed in vacuum, the higher transition temperatures were found to be associated with low ΔQ values ($\Delta Q < 1.5$ cal/g).

D. X-ray and photomicrograph analysis

All x-ray diffraction diagrams taken on mechanically polished GdCu in the temperature region between 5 and 300 K agree completely with the cubic CsCl crystal structure. The obtained diffraction lines are broad, and no resolution is observed in $K\alpha_1$ and $K\alpha_2$ lines which can be ascribed to strains in the sample surface introduced by the polishing. It should be noted that the observed stability of the CsCl crystal structure here is associated with strains in the GdCu surface. The diffraction pattern measured at room temperature on a polished GdCu sample, which was stress released for 1 h in vacuum at 500°C, was also fully consistent with the CsCl crystal structure. Now, however, the diffraction lines are sharp, and the $K\alpha_1$ and $K\alpha_2$ lines are well separated at the higher diffraction angles. A cubic lattice parameter $a = 3.502 \pm 0.001$ Å was determined. After keeping the sample in liquid nitrogen (77 K) for 10 min a room-temperature lattice parameter $a = 3.502 \pm 0.001$ Å is again obtained. Although no change is observed in a , the diffraction lines are now broad and they cannot be resolved into $K\alpha_1$ and $K\alpha_2$ lines. While before cooling the diffraction pattern was fully consistent with the CsCl crystal structure, after cooling additional low-intensity diffractions are observed which clearly originate from the FeB crystal structure described in more detail below. This indicates that, especially for the sample surface, strain annealing plays a very important role in the transformation into the FeB structure. Inspection under the metallographic microscope revealed considerable roughen-

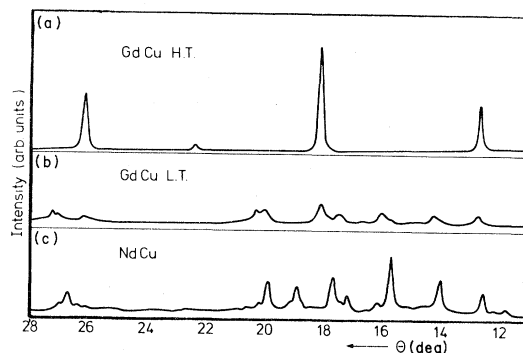


FIG. 10. Room-temperature Bragg diffraction spectra for: (a) GdCu, mechanically polished at room temperature (H.T.), (b) GdCu, crushed into powder at 77 K (L.T.), and (c) NdCu, a good example of the FeB crystal structure.

ing of the sample surface by the development of large numbers of "fringes." It was not possible to estimate a reliable percentage for FeB phase present from our x-ray experiments. After annealing the sample for 1 h at 500°C in vacuum, the room-temperature diffraction pattern again showed sharp lines, which completely agree with the CsCl crystal structure. We also studied a GdCu sample for which a surface layer was removed under liquid nitrogen. Now even though the experimental resolution was rather limited, the room-temperature diffraction pattern could be attributed to the FeB structure.

In Fig. 10 we have collected a number of x-ray diagrams. Part (a) contains the room-temperature spectrum of a polished, not previously cooled GdCu sample which corresponds to that of the CsCl crystal structure. In part (b) the room-temperature spectrum is shown of GdCu which had been crushed into powder under liquid nitrogen. Finally in part (c) the room-temperature spectrum is given for NdCu which was also crushed into powder under liquid nitrogen. NdCu is known to possess the FeB crystal structure.¹ The room-temperature spectrum of GdCu crushed at low temperature [Fig. 10(b)] is very similar to the NdCu spectrum. This indicates that the FeB phase is the majority phase in this low-temperature crushed GdCu powder.

For "nonhysteretic" $\text{GdCu}_{0.94}\text{Ga}_{0.06}$ the Bragg spectra measured at room temperature and liquid-nitrogen temperature are both completely consistent with the CsCl structure. A room-temperature lattice parameter $a = 3.509 \pm 0.001$ Å was determined. Inspection under the microscope at room temperature revealed *no* detectable changes in the sample surface upon cycling to liquid-nitrogen temperature.

IV. DISCUSSION

A. Crystal-structure transformations

Much of the phenomena in the intermetallic compound GdCu considered in Sec. III can be understood in terms of an irreversible crystal-structure transformation at low temperatures from the cubic CsCl structure into the orthorhombic FeB structure. A second possibility that we cannot rule out is a Martensitic transformation of the CsCl structure by a tetragonal distortion. At present, insufficient experimental evidence is available to unambiguously determine which of these two noncubic structures exists at low temperature. For the sake of simplicity we refer to the low-temperature structure as FeB. GdCu is known to form in the CsCl crystal structure at room temperature when prepared from the melt. Let us consider the electrical resistivity results on GdCu in Fig. 1. The negative $d\rho/dT$ behavior, observed in the temperature region between 250 and 130 K, is ascribed to a gradual transformation into the FeB crystal structure. The associated irreversible time-dependent effects can be understood in terms of an activated or transition state.²⁰ At low temperatures both crystal phases (CsCl and FeB) are present. The kneelike anomalies at 48 and 148 K are attributed to the long-range magnetic ordering in the FeB phase and in the CsCl phase, respectively. It was not possible to deduce the volume fractions of the two crystal phases from our resistivity measurements, especially since surface effects may play a major role. From the high-temperature resistivity measurements (Fig. 3) we conclude that at about 600 K the FeB phase fully transforms back into the CsCl phase, which is then the only crystal phase present.

The static susceptibility χ_s versus temperature behavior of GdCu shown in Fig. 4 is typical for a paramagnet down to 232 K. In the temperature region between 232 and 125 K evidence is found in χ_s (Fig. 4) for the CsCl→FeB structure transformation. After the transformation and with both crystal phases present, a linear variation of χ_s^{-1} with increasing temperature is observed above 140 K. Below 140 K deviations from linearity in χ_s^{-1} indicate the onset of magnetic ordering. Further interpretation of the magnetic ordering phenomena in GdCu is difficult since two crystal phases are involved with unknown volume fractions and demagnetization factors.

Additional evidence for the CsCl→FeB structure transformation is found in the anomalous thermal-expansion behavior of GdCu shown in Fig. 7. Here

the transition is observed between 221 and 124 K with a total length increase of 0.5% for the polycrystalline GdCu sample. Consequently, the associated volume increase is 1.5%. These experimental results agree with those reported by Gefen and Rosen.⁶ Note the similarity of the static susceptibility (Fig. 4) and length change behavior (Fig. 7). In both cases a kinklike onset of the transformation is observed with a rapid slowdown in the rate of transformation at lower temperatures.

In our scanning calorimetry measurements on GdCu (see inset in Fig. 9) the occurrence of a latent heat is observed at a well-defined transformation temperature T_s . In order to interpret this behavior we propose that the GdCu remains in the CsCl structure upon cooling down to T_s . At T_s a first-order phase transition from the CsCl structure into the FeB structure occurs instantaneously in a limited volume fraction V_s of the GdCu sample. The associated latent heat $\Delta Q(T_s)$ is given in Fig. 9 for a number of measurements on various GdCu samples. Below T_s a two-phase system is present, and now a gradual further increase of the FeB structure volume fraction takes place with decreasing temperature. A latent heat involved in this *gradual* transformation ($T < T_s$) was not observed within the sensitivity of our calorimetry apparatus. The magnitude of the latent heat $\Delta Q(T_s)$ increases with decreasing transition temperature T_s (Fig. 9), and consequently an increasing volume fraction V_s is involved in the initial transition at the decreased T_s . For the GdCu samples which were heat treated in a He atmosphere, high values for ΔQ and low transition temperatures were observed. This is in agreement with the resistivity behavior, where an initial stepwise rise is observed followed by a gradual increase in ρ . Impurities such as H or He atoms can serve as pinning centers thereby influencing the transformation dynamics. For virginal GdCu samples, high transition temperatures T_s and low ΔQ values were obtained. From this we conclude that only a small percentage of the sample transforms initially at T_s , while the majority of the CsCl→FeB structure transformation occurs gradually with decreasing temperature. This is in accordance with the smooth negative $d\rho/dT$ dependence observed in the resistivity (Fig. 1). In the region with negative $d\rho/dT$, a time dependence was found, which implies a gradual occurrence with time of the structure transformation.

Since the CsCl→FeB transformation in GdCu takes place at relatively low temperatures, it is unlikely that large and homogeneous FeB crystals will develop. Instead we expect that with decreasing

temperature the transformation will start with the initial formation at T_s of tiny imperfect FeB crystals within the polycrystalline CsCl phase. This formation process will be accompanied by considerable structural disorder of the lattice. Therefore, we expect that the structure transformation will be retarded through the associated buildup of internal (or externally applied) pressure. This explains why, on cooling below T_s , the further CsCl→FeB transformation occurs gradually over an extended temperature region. At low temperatures the transformation stops due to the lack of thermal activation. It is interesting to note that via the resistivity, susceptibility, and thermal-expansion measurements we observed an enormous temperature hysteresis of the transformation extending over more than 400 K. We suggest that this hysteretic behavior is associated with the lattice disorder. Such disorder was also observed by us via standard photometallography (the large grains of starting material had decomposed into an assembly of finely divided subgrains upon low-temperature cycling). In addition we propose that the transformation back into the CsCl phase as observed in the resistivity behavior of GdCu at about 600 K (Fig. 3) is essentially an annealing of the lattice disorder accompanied by stress releasing. It is well known that for the latter processes temperatures of this order of magnitude are commonly required.²⁰

No evidence is found for the FeB phase in the Bragg diffraction spectra obtained on mechanically polished bulk GdCu in the temperature region between 5 and 300 K [Fig. 10(a) above]. This is apparently due to pinning of the CsCl crystal phase by strains and dislocations in the sample surface which are introduced via the polishing technique. The x-ray results are dominated by surface effects due to the limited penetration depth of the x rays, especially in Gd samples.²¹ So, even though the CsCl→FeB transformation takes place within the bulk, this change of structure is not observed at the surface regions. In contrast, after strain-free annealing, the irreversible CsCl into FeB transformation is observed via Bragg diffraction on the GdCu surface. This surface effect prevents a reliable estimate of the percentage FeB phase present within the bulk. The micrograph fringes observed on the GdCu sample surface originate from the 1.5% volume increase during the structure transformation. The x-ray and photomicrograph observations reported by Gefen and Rosen⁶ disagree with our findings. This is probably due to the presence of strain and pinning effects also introduced into their

surface layers by mechanical polishing. In order to clearly see the fringelike structure in our photomicrographs, a strain-free annealing treatment (a few hours at 500°C) was required after the mechanical polishing. The high-temperature transformation of the FeB phase fully back into the CsCl phase is also observed via the x-ray diffraction. Further evidence for the difference in properties between the bulk and the surface was found in the x-ray experiment on GdCu, where a surface layer was removed at liquid-nitrogen temperature and then the spectrum corresponding to the FeB crystal structure was found. The room-temperature Bragg spectrum obtained on GdCu crushed into powder at liquid-nitrogen temperature [Fig. 10(b)] clearly reveals the FeB structure. We remark that the above behavior is consistent with an irreversible CsCl→FeB structure transformation at low temperatures; however, experimental complications arise from pinning and surface effects. Our Bragg diffraction experiments on 20–40- μm GdCu powder suggest that the CsCl crystal phase is maintained over the whole temperature range studied. This is in agreement with the work of Ross and Sigalas.⁵ Finally we note that in CdCu, when prepared as powder, splat cooled, or at sample surfaces, the observed stability of the CsCl crystal structure is caused by pinning effects due to impurities, lattice imperfections, and strains.

The resistivity behavior for $\text{GdCu}_{1-x}\text{Ga}_x$ with $0 \leq x \leq 0.03$ (Fig. 1) shows a rapid decrease of the structure-transformation temperature with increasing Ga concentration. The onset of the negative dp/dT dependence, at 250 K for GdCu, which is a good measure for the transformation temperature T_s , is plotted versus Ga concentration in Fig. 11. At temperatures below 120 K no structural anomaly is observed in the resistivity behavior. This is attributed to a lack of thermal activation energy for further structural transformation. The resistivity anomaly, at 48 K for GdCu, becomes less pronounced with increasing Ga concentration, and this is ascribed to a decreasing volume fraction of FeB phase. Also in Fig. 11 the magnetic ordering temperatures, determined via the resistivity behavior, T_0 for the CsCl phase and T_M for the FeB phase, are plotted versus Ga concentration. Similar to the electrical resistivity behavior, the suppression of the structure transformation is also observed in the magnetic susceptibility of $\text{GdCu}_{1-x}\text{Ga}_x$ for $x \leq 0.03$. In Fig. 11 the measured paramagnetic Curie temperatures of the high-temperature CsCl phase (thick solid line) and of the low-temperature transformed phase (dashed line) are given. The con-

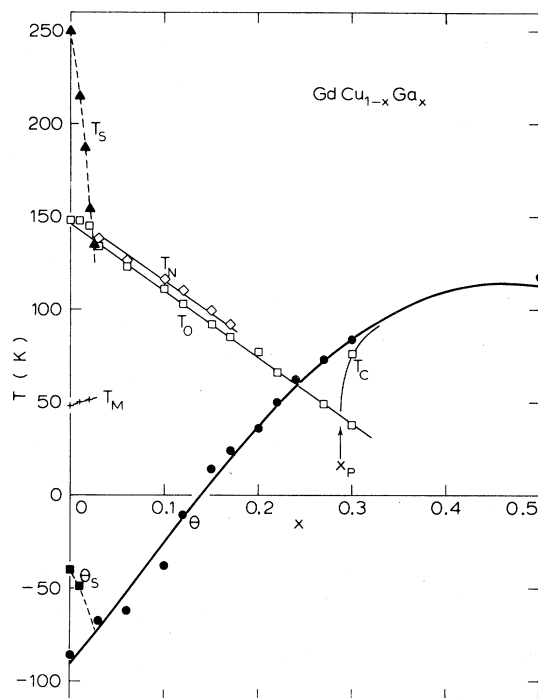


FIG. 11. Structural and magnetic phase diagram for the $\text{GdCu}_{1-x}\text{Ga}_x$ system. T_s is the CsCl \rightarrow FeB structure transformation temperature. T_M is the magnetic ordering temperature of the FeB phase. Θ_s is the paramagnetic Curie temperature of the partially transformed (CsCl + FeB) phase. T_N , T_0 , and T_c are the magnetic ordering temperatures (see text) of CsCl structure $\text{GdCu}_{1-x}\text{Ga}_x$. x_p denotes a percolation concentration (see text). Θ is the paramagnetic Curie temperature of CsCl structure $\text{GdCu}_{1-x}\text{Ga}_x$. The thick solid line represents the model fit to the data (see text). All other lines serve as a guide for the eye.

vergence of the paramagnetic Curie temperatures at $x=0.03$ is ascribed again to a decreasing volume fraction of FeB phase. The rapid variation of the transformation temperature T_s with Ga concentration is attributed to the valency difference between Cu and Ga. Since Ga provides two additional conduction electrons, a strong influence on the electronic band structure and position of the Fermi level is expected. The similarity of the resistivity behavior of $\text{YCu}_{1-x}\text{Ga}_x$ and $\text{GdCu}_{1-x}\text{Ga}_x$, excluding the magnetic anomalies, leads to the same interpretation in terms of a crystal-structure transformation. Also in $\text{YCu}_{1-x}\text{Ga}_x$ a stabilization of the CsCl crystal structure is found at $x=0.03$. The resistivity behavior of YCu has been already reported by Balster *et al.*⁷ who also performed x-ray diffraction measurements. Their interpretation for

YCu concerning the surface effects and crystal structures is very similar to ours for GdCu, which gives further support for the similarity of $\text{YCu}_{1-x}\text{Ga}_x$ and $\text{GdCu}_{1-x}\text{Ga}_x$ from a crystal-structure point of view.

B. Magnetic order phenomena

In $\text{GdCu}_{1-x}\text{Ga}_x$ with $0.03 \leq x \leq 0.50$ the CsCl crystal structure is stable and consequently all anomalous behavior must now be attributed to magnetic ordering phenomena. Note that additional support for the magnetic nature of the observed anomalies comes from the resistivity results on $\text{Gd}_{1-y}\text{Y}_y\text{Cu}_{0.9}\text{Ga}_{0.1}$, where with decreasing Gd concentration a gradual decrease in magnitude and temperature of the negative $d\rho/dT$ anomaly is observed. In Fig. 11 we have plotted the paramagnetic Curie temperatures Θ versus x for $\text{GdCu}_{1-x}\text{Ga}_x$, as obtained from the static susceptibility measurements (Fig. 5). The Θ value for $x=0.5$ was taken from Ref. 4. In the $\Theta(x)$ dependence a change of sign is observed at $x \approx 0.14$. From this we conclude that in the paramagnetic state the weighted average of the exchange interactions is antiferromagnetic for $x < 0.14$ and ferromagnetic for $x > 0.14$. Nevertheless we ascribe all kinklike anomalies observed in $\chi^{-1}(T)$ for $0.03 \leq x \leq 0.17$ (see arrows in Fig. 5) to long-range antiferromagnetic ordering. In Fig. 11 the antiferromagnetic ordering temperatures T_N determined from these anomalies are plotted versus x . At $x \approx 0.14$, where $\Theta \approx 0$, magnetic ordering temperatures $T_N \approx 100$ K are observed in $\text{GdCu}_{1-x}\text{Ga}_x$. Heat-capacity measurements reported by Buschow *et al.*¹³ for $0.10 \leq x \leq 0.15$ in the temperature range below 20 K show no magnetic ordering phenomena. This means that $T_N \gg \Theta$ and, consequently, even though $\Theta \approx 0$, large ferromagnetic as well as large antiferromagnetic Gd-Gd interactions must be present. We propose that these different magnetic interactions for different pairs of Gd atoms in $\text{GdCu}_{1-x}\text{Ga}_x$ depend on the configuration of Ga and Cu atoms surrounding the Gd-Gd interconnection line. For $x \approx 0.14$ the weighted average of the interactions is zero ($\Theta \approx 0$), while the magnetic ordering processes occur at temperatures corresponding to the absolute value of the magnetic interactions ($T_N \approx 100$ K).¹³ It is evident that the observed kinklike anomalies do not represent a simple type of antiferromagnetic long-range ordering.

In the electrical resistivity versus temperature curves for $\text{GdCu}_{1-x}\text{Ga}_x$ with $x \geq 0.03$ (Figs. 1 and

2), a reversible negative $d\rho/dT$ contribution is observed. The temperatures T_0 with minimum $d\rho/dT$ are plotted versus x in Fig. 11. For the lower x values, $0.03 \leq x \leq 0.17$, a very similar $T_0(x)$ and $T_N(x)$ dependence is observed, see Fig. 11. Suezaki and Mori²² have treated theoretically the electrical resistivity versus temperature behavior near the antiferromagnetic ordering temperature T_N . When employing the Suezaki-Mori theory for the present system, one should take into account the relative strengths of band-gap and spin-fluctuation contributions to the $\rho(T)$ behavior. These contributions are expected to vary significantly over the large x range shown in Fig. 2, thus producing the changes in the $\rho(T)$ behavior. In their theory the electrical resistivity turns out to have a rounded peak near T_N , whose maximum lies below T_N and whose temperature derivative *negatively* diverges at T_N . Therefore, we consider T_0 (minimum in $d\rho/dT$) as a good measure of the long-range antiferromagnetic ordering temperature. For more recent theoretical work on anomalous resistivity behavior at magnetic ordering temperatures, we refer to Ausloos and Durczewski²³ and references therein. The nature of the magnetic order in $\text{GdCu}_{1-x}\text{Ga}_x$, especially for $0.17 < x < 0.29$, will be discussed in more detail below. At $x=0.30$ a considerable change is observed in the $\rho(T)$ behavior (Fig. 2). Here at a temperature T_c an additional kneelike anomaly is detected in $\rho(T)$, which is also

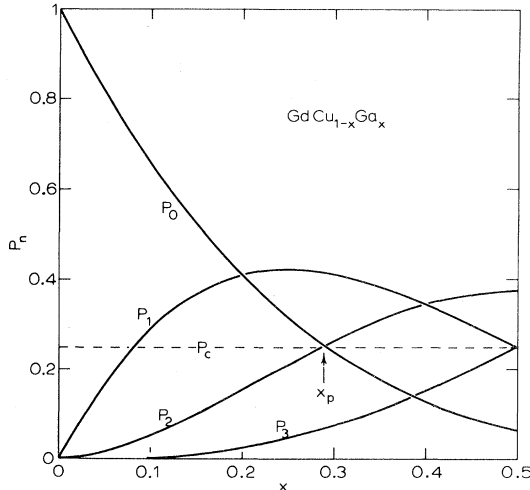


FIG. 12. Probability functions P_n vs x for the occupancy of n Ga atoms surrounding the interconnection line of two Gd sites in CsCl structure $\text{GdCu}_{1-x}\text{Ga}_x$. P_c is the critical bond probability for a simple cubic lattice. x_p denotes the percolation concentration (see text).

TABLE I. Probability functions for the occupancy of n Ga atoms surrounding the interconnection line of two Gd sites and the resulting Gd-Gd exchange interaction.

n	P_n	J_n (K)
0	$(1-x)^4$	-90
1	$4x(1-x)^3$	+65
2	$6x^2(1-x)^2$	+320
3	$4x^3(1-x)$	-70
4	x^4	0

plotted in Fig. 11. For $\text{GdCu}_{0.70}\text{Ga}_{0.30}$ we propose a long-range ferromagnetic ordering at $T_c=76$ K, followed by an antiferromagnetic “canting” beginning at $T_0=38$ K. A critical “percolation” concentration $x_p \approx 0.29$ can be defined for $\text{GdCu}_{1-x}\text{Ga}_x$, see below. With $x < x_p$ a linear decrease of the magnetic ordering temperature T_0 with increasing Ga concentration x is observed. At $x_p \approx 0.29$ the onset of long-range ferromagnetic ordering commences. For $x \geq x_p$ there is an initial sharp rise of the ferromagnetic ordering temperature T_c , and at higher x values ($x > 0.3$) a $T_c \propto \Theta$ dependence is followed.

For $\text{GdCu}_{1-x}\text{Ga}_x$ in the CsCl crystal structure the Gd atoms occupy a simple cubic lattice and each Gd-Gd interconnection line is surrounded by four Cu or Ga atoms. When considering only the number of Ga atoms n , there are five possible configurations of surrounding Cu and Ga atoms, which we label $n=0-4$. In Table I the relations of the x dependence for the corresponding random probabilities P_n ($n=0-4$) are given. In Fig. 12 we plotted $P_n(x)$ for $n=0-3$ in the concentration region $0 \leq x \leq 0.5$. As a first approximation we develop a simple model by taking into account only nearest-neighbor magnetic interactions. Moreover, in our model the Gd-Gd interaction parameters J_n ($n=0-4$) only depend on the number n of Ga atoms surrounding the Gd-Gd interconnection line. This means that the magnetic interactions are fully determined by the local surrounding. The paramagnetic Curie temperature Θ is then given by the expression

$$\Theta = \sum_{n=0}^4 P_n J_n. \quad (1)$$

For a system with only one type of magnetic interaction J , this implies $\Theta=J$. $\text{GdCu}_{1-x}\text{Ga}_x$ in the concentration region of interest, $0 \leq x \leq 0.5$, has only a small number of Gd-Gd interconnection lines surrounded by four Ga atoms. Therefore, we neglect the associated magnetic interactions by set-

ting $J_4=0$ in Eq. (1). With the use of a computer program, $\Theta(x)$ from Eq. (1) was least-squares fitted to the experimentally determined, paramagnetic Curie temperatures of CsCl structure $\text{GdCu}_{1-x}\text{Ga}_x$, with $0 \leq x \leq 0.5$, and this is plotted in Fig. 11 by the thick solid line. The resulting values for the fitting parameters J_n ($n=0-3$) are listed in Table I, together with the $J_4=0$ assumption. Note the physical relevance of the large ferromagnetic J_2 interaction parameter, since for the isoelectronic compound GdZn a ferromagnetic ordering temperature $T_c=270$ K is reported.¹

In order to better understand the long-range ordering phenomena in $\text{GdCu}_{1-x}\text{Ga}_x$ we proceed with this simplified magnetic interaction scheme with nearest-neighbor Gd-Gd interactions J_n ($n=0-4$), which depend only on the local surrounding. By considering the simple cubic Gd sublattice the long-range ordering phenomena can be treated as a bond percolation problem. For a simple cubic lattice the critical percolation probability $P_c=0.25$,²⁴ which we indicated in Fig. 12. Note that both probability functions $P_0(x)$ and $P_2(x)$ fortuitously cross P_c at nearly the same critical concentration $x_p=0.29$. For $x \geq 0.29$ the probability functions $P_1(x)$ and $P_2(x)$ are both above the percolation limit P_c , while Table I reveals $|J_2| \gg |J_{n \neq 2}|$. Therefore, long-range ferromagnetic ordering is expected for $x \geq 0.29$, which originates from the strong $J_2 = +320$ K interactions. This agrees with the experimentally determined magnetic phase diagram of $\text{GdCu}_{1-x}\text{Ga}_x$ (Fig. 11), where at $x_p \simeq 0.29$ a sharp rise of the ferromagnetic ordering temperature T_c is observed, followed by a $T_c \propto \Theta$ dependence, which is typical for ferromagnetism at higher x values ($x > 0.3$). In the temperature dependence of the electrical resistivity for $x=0.30$, the kneelike ferromagnetic $\rho(T)$ anomaly at $T_c=76$ K is followed by an anomalous minimum $d\rho/dT$ behavior at $T_0=38$ K, see Fig. 2. Moreover, in the low-field (1 Oe) dynamical susceptibility of $\text{GdCu}_{0.7}\text{Ga}_{0.3}$, a cusplike anomaly was also detected at 38 K (Fig. 6). We ascribe this 38-K anomaly to reordering of the ferromagnetic state into a low-temperature magnetic state with a small antiferromagnetic component. This antiferromagnetic component originates from the relatively small, but negative J_0 and J_3 interactions (Table I), which are present in considerable amounts. The antiferromagnetic component is expected to be suppressed in high magnetic fields. This was actually observed, since at 38 K no anomaly was detected in the high-field (4 kOe) static susceptibility (Fig.

5). A similar behavior was found for alloys which transform from ferromagnetic long-range order into a spin-glass frozen state as the temperature is lowered.²⁵

To describe the magnetic ordering phenomena in $\text{GdCu}_{1-x}\text{Ga}_x$ with $x < 0.29$ we have to consider the three magnetic interaction parameters J_0 , J_1 , and J_2 , see Fig. 12 and Table I. Since J_3 - and J_4 -type interactions are present only in very small amounts, we can safely neglect their influence here. For $x < 0.29$ the strong J_2 -type interactions can only result in short-range ferromagnetic ordering or clustering because $P_2 < P_c$. These ferromagnetic clusters are expected to increase in number and size with increasing x . The magnetic coupling among these ferromagnetic clusters occurs through the J_0 and J_1 interactions. In the concentration region $0.03 \leq x \leq 0.17$ the long-range ordering will be dominated by the J_0 -type magnetic interactions because $|P_0J_0| \gg |P_1J_1|$. Consequently, long-range antiferromagnetic ordering is expected in this x region. Since the strong ferromagnetic J_2 -type interactions are present in relatively small amounts here, we expect only a minor influence from them on the magnetic properties. As a typical example in the $0.03 \leq x \leq 0.17$ concentration region, consider the temperature dependence of the dynamic susceptibility of $\text{GdCu}_{0.94}\text{Ga}_{0.06}$. The kinklike anomaly at $T_N=126$ K is ascribed to the already mentioned antiferromagnetic ordering. Furthermore, at about 80 K (see Fig. 6) the onset of a strongly enhanced low-field (1 Oe) dynamic susceptibility was observed. This effect is ascribed to canting leading to a small ferromagnetic component in the antiferromagnetically ordered structure. This small ferromagnetic component is observed to saturate in relatively low (100 Oe) magnetic fields, thus giving the observed field dependence of the susceptibility as measured in 1 Oe and 4 kOe. Since in this x region the relative weights of the ferromagnetic J_1 - and J_2 -type interactions are rather weak, they are not capable of explaining the observed behavior. We suggest that there exists an intrinsic magnetic anisotropy probably associated with the $5d$ electrons of the Gd, which leads to homogeneous ferromagnetic canting in $\text{GdCu}_{1-x}\text{Ga}_x$ for $0.03 \leq x \leq 0.17$. The decrease of the dynamic susceptibility at very low temperatures ($T < 30$ K), see Fig. 6, is attributed to the onset of magnetic domain and hysteresis effects.

A still more complicated magnetic order in $\text{GdCu}_{1-x}\text{Ga}_x$ is expected for $0.17 < x < 0.29$, since then our simple nearest-neighbor interaction model gives $|P_0J_0| \simeq |P_1J_1|$. Therefore, we suggest here

a mixed, intermediate type of long-range magnetic order. The experimental behavior of the susceptibility and resistivity do not justify describing this concentration region as a spin glass. As P_2 approaches P_c near $x < 0.29$, see Fig. 12, an increasing influence is expected from the strong J_2 -type interactions. The low-temperature shoulder observed in the dynamic susceptibility (Fig. 6) is ascribed to an increasing influence of the ferromagnetic J_1 - and J_2 -type interactions with increasing x . The increasing ferromagnetic character in $\text{GdCu}_{1-x}\text{Ga}_x$ is also observed through the increasing static susceptibility of the ordered state (Fig. 5). Since $P_n < P_c$ for $n \geq 2$ in the whole concentration region $0.03 \leq x < 0.29$, the long-range magnetic order is dominated by the $J_0 = -90$ K and $J_1 = +65$ K type interactions. The smooth x dependence of the magnetic ordering temperature T_0 is in accord with the comparable strength of these magnetic interactions $|J_0| \simeq |J_1|$.

Fishman and Aharony²⁶ have studied within the mean-field approximation the properties of a quenched random alloy of a ferromagnet and a two-sublattice antiferromagnet. In their study they confine themselves to bond randomness, where the coupling between the spins is a random variable. This type of randomness is realized experimentally, e.g., in $\text{GdCu}_{1-x}\text{Ga}_x$ in the present investigation, by mixing materials with identical magnetic ions on A sites with different types of nonmagnetic atoms on B sites. The latter atoms mediate the exchange interactions. In this theory more than one antiferromagnetic order parameter is necessary and these are then transformed into combinations of order parameters in order to investigate the possibility that ferromagnetic and antiferromagnetic orderings occur simultaneously. It is demonstrated that, if only nearest-neighbor interactions are assumed, ferromagnetic, antiferromagnetic, and spin-glass phases are expected at low temperatures. If, however, the strength of the next-nearest-neighbor interactions is increased, the ferromagnetic and the antiferromagnetic phases approach each other and concentration regions arise where a mixed ferromagnetic-antiferromagnetic phase exists. In order to understand this behavior the following intuitive argument is presented²⁶: The nearest-neighbor interactions are the interactions between the sublattices, while the next-nearest-neighbor interactions are the interactions between the spins in the same sublattice; thus the possibility exists for both ferromagnetic and antiferromagnetic ordering.

For $\text{GdCu}_{1-x}\text{Ga}_x$ in the intermediate-

concentration region $0.17 < x < 0.29$, the field and temperature dependence of the dynamic susceptibility is not typical for spin-glass freezing behavior.²⁷ Therefore, we suggest for this intermediate region a canted or mixed ferromagnetic-antiferromagnetic state for the long-range ordered Gd moments. Following the above-mentioned theoretical studies²⁶ we need to incorporate next-nearest-neighbor interactions into our simplified nearest-neighbor interaction model in order to understand the observed behavior. From our macroscopic measurements it is not possible to deduce the relative strength of these next-nearest-neighbor interactions or to determine to which degree the canted magnetic state is disturbed on an atomic level through the local Cu and Ga surroundings. Neutron scattering measurements are essential here to determine the exact form of the magnetic order. As a basis for comparison we refer to magnetic studies performed on $\text{GdAg}_{1-x}\text{Zn}_x$,¹⁶ $\text{GdAg}_{1-x}\text{In}_x$,²⁸ and $\text{GdCu}_{1-x}\text{Zn}_x$.²⁹ These systems show static susceptibility curves which are very similar to our results. For the $\text{GdAg}_{1-x}\text{Zn}_x$ and $\text{GdCu}_{1-x}\text{Zn}_x$ series, the magnetic phase diagrams were basically similar to ours when scaled for the extra conduction electron of Ga.

V. SUMMARY

In this paper results are presented of measurements of the electrical resistivity, the low-field dynamic (ac) susceptibility, the static (4 kOe) susceptibility, and the thermal expansion. Data obtained with scanning calorimetry, x-ray diffraction, and photomicrograph examinations are also reported. The investigations were performed on the pseudobinary compounds $\text{GdCu}_{1-x}\text{Ga}_x$, $\text{YCu}_{1-x}\text{Ga}_x$, and $\text{Gd}_{1-y}\text{R}_y\text{Cu}$ ($R = \text{Sm}$ or Tm).

The compounds $\text{GdCu}_{1-x}\text{Ga}_x$ with $0 \leq x \leq 0.5$ form in the cubic CsCl crystal structure at room temperature when prepared from the melt. On cooling, the compounds with $0 \leq x < 0.03$ exhibit a crystal-structure transformation at 250 K for GdCu, into a low-temperature noncubic phase. This transformation is associated with considerable structural disorder and stresses which manifest themselves in the development of fringes at the sample surface. An enormous hysteresis cycle is observed with the transformation back into the CsCl structure occurring around 600 K. We suggest that this high-temperature transformation is essentially accompanied by a stress-releasing process. The low-temperature structure transformation

properties exhibit a strong dependence on the exact history of the sample preparation and heat treatment, e.g., for polycrystalline GdCu prepared by splat cooling the transformation was completely suppressed. The variation of the structure transformation temperature as observed in $\text{Gd}_{1-y}\text{R}_y\text{Cu}$ ($\text{R}=\text{Sm}$ or Tm) was found to be consistent with the cubic CsCl structure of TmCu and the orthorhombic FeB structure of SmCu. In $\text{YCu}_{1-x}\text{Ga}_x$ with $0 \leq x < 0.03$ low-temperature resistivity phenomena were observed similar to the results on $\text{GdCu}_{1-x}\text{Ga}_x$. This leads to the same interpretation in terms of a crystal-structure transformation.

The stable CsCl structure compounds of $\text{GdCu}_{1-x}\text{Ga}_x$ with $0.03 \leq x \leq 0.50$ are shown to exhibit a complicated magnetic ordering behavior. For $0.03 \leq x \leq 0.17$ a kinklike anomaly is observed in the magnetic susceptibility, which is ascribed to antiferromagnetic ordering. Around 40 K a strongly enhanced low-field dynamic susceptibility is detected which is attributed to a small ferromagnetic canting of the antiferromagnetically ordered structure. We suggest that the canting observed for the lower Ga concentrations is homogeneous and originates from an anisotropy associated with the 5d conduction electrons which are present in Gd and which mediate the exchange interactions. For higher Ga concentrations the kinklike anomaly becomes submerged in the increasing ferromagnetic character of the susceptibility. A mixed ferromagnetic-antiferromagnetic or canted magnetic structure is suggested at low temperatures for the ordered Gd moments in the intermediate concentration region $0.17 < x < 0.29$. We have no experimental evidence for spin-glass behavior in the concentration region. It was not possible to deduce from our measurements to which degree the canted magnetic state is formed on an atomic level through the

local Cu and Ga surroundings. For $x \geq 0.29$ ferromagnetic long-range order is found. This could be understood in terms of a simple nearest-neighbor bond percolation model. Over the whole $0.03 \leq x < 0.29$ concentration region a negative temperature coefficient is observed in the measured electrical resistivity near the ordering temperature, further indicating an antiferromagnetic-type of long-range order. A simple model with only nearest-neighbor magnetic interactions, depending on the local Cu and Ga surroundings, is proposed to describe the x dependence of the paramagnetic Curie temperature. In order to treat the proposed canted spin structure, which modifies both the ferromagnetic and antiferromagnetic low-temperature states near the ferromagnetic percolation concentration, we would have to incorporate next-nearest-neighbor interactions into our simplified nearest-neighbor interaction model. Finally, a structural and magnetic phase diagram is constructed for the $\text{GdCu}_{1-x}\text{Ga}_x$ system with $0 \leq x \leq 0.5$.

ACKNOWLEDGMENTS

We wish to acknowledge stimulating discussions with Dr. G. J. Nieuwenhuys and to thank A. C. Moleman and T. J. Gortenmulder for their assistance with the x-ray diffraction and micrograph investigations. This work is part of the research program of the Stichting voor Fundamenteel Onderzoek der Materie (Foundation for Fundamental Research on Matter) and was made possible by financial support from the Nederlandse Organisatie voor Zuiver-Wetenschappelijk Onderzoek (Netherlands Organization for the Advancement of Pure Research).

¹K. H. J. Buschow, Rep. Prog. Phys. **42**, 1373 (1979).

²H. R. Kirchmayer and C. A. Poldy, in *Handbook on the Physics and Chemistry of Rare Earths*, edited by K. A. Gschneider, Jr. and L. Eyring (North-Holland, Amsterdam, 1979), Vol. 2.

³A. Iandelli and A. Palenzona, in *Handbook on the Physics and Chemistry of Rare Earths*, edited by K. A. Gschneider, Jr. and L. Eyring (North-Holland, Amsterdam, 1979), Vol. 2.

⁴H. W. de Wijn, K. H. J. Buschow, and A. M. van Diepen, Phys. Status Solidi **30**, 759 (1968).

⁵J. W. Ross and J. Sigalas, J. Phys. F **5**, 1973 (1975).

⁶Y. Gefen and M. Rosen, Scr. Metall. **14**, 645 (1980); J. Phys. Chem. Solids **42**, 857 (1981).

⁷H. Balster, H. Ihrig, A. Kockel, and S. Methfessel, Z. Phys. B **21**, 241 (1975).

⁸A. Palenzona and S. Cirafici, Thermochim. Acta **12**, 267 (1975).

⁹O. D. McMasters, K. A. Gschneider, Jr., G. Bruzzone, and A. Palenzona, J. Less-Common Met. **25**, 135 (1981).

¹⁰D. Debray, B. F. Wortmann, and S. Methfessel, Phys. Rev. B **14**, 4009 (1976).

¹¹C. W. Kimball, A. E. Dwight, G. M. Kalvius, B. Dun-

- lap, and M. V. Nevitt, *Phys. Rev. B* **12**, 819 (1975).
- ¹²H. Peukert and J. S. Schilling, *Z. Phys. B* **41**, 217 (1981).
- ¹³K. H. J. Buschow, J. R. Olijhoek, and A. R. Miedema, *Cryogenics* **15**, 261 (1975).
- ¹⁴M. Belakhovsky, J. Pierre, and D. K. Ray, *Phys. Rev. B* **6**, 939 (1972).
- ¹⁵A. Hasegawa and J. Kübler, *Z. Phys.* **269**, 31 (1974).
- ¹⁶U. Köbler, W. Kinzel, and W. Zinn, *J. Magn. Magn. Mater.* **25**, 124 (1981).
- ¹⁷For a more detailed account of this work see J. C. M. van Dongen, Ph.D. thesis, University of Leiden, 1982 (unpublished).
- ¹⁸A. F. J. Morgownik and J. A. Mydosh, *Phys. Rev. B* **24**, 5277 (1981).
- ¹⁹G. Brändli and R. Griessen, *Cryogenics* **13**, 299 (1973).
- ²⁰K. H. J. Buschow, *J. Appl. Phys.* **52**, 3319 (1981).
- ²¹*X-Ray Metallography*, edited by A. Taylor (Wiley, New York, 1961).
- ²²Y. Suezaki and H. Mori, *Prog. Theor. Phys.* **41**, 1177 (1969).
- ²³M. Ausloos and K. Durczewski, *Phys. Rev. B* **22**, 2439 (1980).
- ²⁴V. K. S. Shante and S. Kirkpatrick, *Adv. Phys.* **20**, 325 (1971).
- ²⁵Y. Yeshurun, K. V. Rao, M. B. Salamon, and H. S. Chen, *J. Appl. Phys.* **52**, 1747 (1981).
- ²⁶S. Fishman and A. Aharony, *Phys. Rev. B* **19**, 3776 (1979); **21**, 280 (1980).
- ²⁷J. A. Mydosh and G. J. Nieuwenhuys, in *Handbook of Ferromagnetic Materials*, edited by E. P. Wohlfarth (North-Holland, Amsterdam, 1980), Vol. 1, Chap. 2.
- ²⁸K. Sekizawa and K. Yasukochi, *Phys. Lett.* **11**, 216 (1964).
- ²⁹K. Takei, Y. Ishikawa, N. Watanabe, and K. Tajima, *J. Phys. Soc. Jpn.* **47**, 88 (1979).